Optimal characterization of Gaussian channels using photon-number-resolving detectors

Chandan Kumar ,[1,*] Ritabrata Sengupta [2,†] and Arvind [1,‡]

[1]*Department of Physical Sciences, Indian Institute of Science Education and Research (IISER) Mohali,
Sector 81 SAS Nagar, Manauli PO 140306, Punjab, India*

[2]*Department of Mathematical Sciences, Indian Institute of Science Education and Research (IISER) Berhmampur,
Transit Campus, Government ITI, Berhampur 760 010, Odisha, India*

We present optimal schemes, based on photon-number measurements, for Gaussian state tomography and for Gaussian process tomography. An n-mode Gaussian state is completely specified by $2n^2 + 3n$ parameters. Our scheme requires exactly $2n^2 + 3n$ distinct photon-number measurements to tomograph the state and is therefore optimal. Furthermore, we describe an optimal scheme to characterize Gaussian processes by using coherent-state probes and photon-number measurements. With much recent progress in photon-number-measurement experimental techniques, we hope that our scheme will be useful in various quantum information processing protocols including entanglement detection, quantum computation, quantum key distribution, and quantum teleportation. This work builds upon the work of Parthasarathy and Sengupta [Infin. Dimens. Anal. Quantum Probab. Relat. Top. **18**, 1550023 (2015)].

I. INTRODUCTION

Continuous-variable (CV) systems are ubiquitous in quantum information and communication protocols. Most of the CV quantum information protocols are based on Gaussian states as they are easy to prepare, manipulate, and measure [1,2]. One of the central tasks in quantum information processing is the estimation of quantum states, which is formally called quantum state tomography (QST) [3–5]. Generally, homodyne and heterodyne measurements are employed in CV QST, which measure quadrature operators of a given state [6–8]. However, with the recent development of experimental techniques in photon-number-resolving detectors (PN-RDs) [9,10], the possibility of carrying out QST via photon-number measurements has opened up. Cerf *et al.* devised a scheme using beam splitters and on-off detectors, where one can obtain the trace and determinant of the covariance matrix of a Gaussian state [11,12]. In a similar endeavor, Parthasarathy *et al.* have developed a theoretical scheme to determine the Gaussian state by estimating its mean and covariance matrix [13].

Another important task in quantum information processing is quantum process tomography (QPT), where we wish to characterize quantum processes which in general are completely positive maps. For CV systems, theoretical as well as experimental studies for QPT have been undertaken by several authors [14–23]. Lobino *et al.* used coherent-state probes along with homodyne measurements to characterize quantum processes [14]. Similarly, Ghalaii *et al.* have developed a coherent-state-based QPT scheme via the measurement of

normally ordered moments that are measured using homodyne detection [21]. In this direction, Parthasarathy *et al.* have utilized QST schemes based on photon-number measurements for Gaussian states, to characterize the Gaussian channel [13].

In this paper, we simplify the scheme given by Parthasarathy *et al.* [13] and describe an optimal scheme which involves a minimum number of measurements and utilizes a smaller number of optical elements for the QST of Gaussian states based on PNRDs. We employ this scheme to devise an optimal scheme for Gaussian channel characterization. An n-mode Gaussian state is completely specified by its $2n$ first moments and second-order moments arranged in the form of a covariance matrix which has $2n^2 + n$ parameters. Therefore, we require a total of $2n^2 + 3n$ parameters to completely determine an n-mode Gaussian state. The QST based on photon-number measurements is optimal in the sense that we require exactly $2n^2 + 3n$ distinct measurements to determine all the $2n^2 + 3n$ parameters of the state. Next we deploy the QST scheme that we develop, to estimate the output, with coherent-state probes as inputs for the Gaussian channel characterization. An n-mode Gaussian channel is described by a pair of $2n \times 2n$ real matrices A and B with $B = B^T \geqslant 0$ which satisfy certain complete positivity and trace-preserving conditions [24–26]. The matrices A and B together can be described by a total of $6n^2 + n$ parameters. We show that we can characterize a Gaussian quantum channel optimally; i.e., we require exactly $6n^2 + n$ distinct measurements to determine all the $6n^2 + n$ parameters of the Gaussian channel. We compare the variance of transformed number operators arising in the aforementioned QST scheme which provides an insight into the efficiency of the scheme. Finally, we relate the variance of transformed number operators to the variance of quadrature operators. In CV quantum key distribution (QKD) protocols, one needs to send an intense local oscillator pulse for the purpose of measurement, which in itself is an arduous

---

*chandankumar@iisermohali.ac.in
†rb@iiserbpr.ac.in
‡arvind@iisermohali.ac.in

task and can give rise to security loopholes [27,28]. Our scheme based on PNRDs do not require such an intense local oscillator signal, and thus may turn out to be useful in CV QKD protocols.

The paper is organized as follows. In Sec. II we give a detailed mathematical background about CV systems. In Sec. III we provide our optimal QST scheme based on PNRDs for Gaussian states. Thereafter, the tomography of the Gaussian channel has been dealt with in Sec. IV while in Sec. V we compare the variance of different transformed number operators appearing in the state tomography scheme. Finally in Sec. VI we draw conclusions from our results and look at future aspects.

II. CV SYSTEM

An n-mode continuous-variable quantum system is represented by n pairs of Hermitian quadrature operators $\hat{q}_i, \hat{p}_i$ $(i = 1, \ldots, n)$ which can be arranged in a column vector as [1,2,29–31]

$$\hat{\boldsymbol{\xi}} = (\hat{\xi}_i) = (\hat{q}_1, \hat{p}_1, \ldots, \hat{q}_n, \hat{p}_n)^T, \quad i = 1, 2, \ldots, 2n. \quad (1)$$

The bosonic commutation relation between them in a compact form reads as ($\hbar = 1$)

$$[\hat{\xi}_i, \hat{\xi}_j] = i\Omega_{ij}, \quad i, j = 1, 2, \ldots, 2n, \quad (2)$$

where Ω is the $2n \times 2n$ matrix given by

$$\Omega = \bigoplus_{k=1}^n \omega = \begin{pmatrix} \omega & & \\ & \ddots & \\ & & \omega \end{pmatrix}, \quad \omega = \begin{pmatrix} 0 & 1 \\ -1 & 0 \end{pmatrix}. \quad (3)$$

The field annihilation and creation operators $\hat{a}_i$ and $\hat{a}_i^\dagger$ $(i = 1, 2, \ldots, n)$ are related to the quadrature operators as

$$\hat{a}_i = \frac{1}{\sqrt{2}}(\hat{q}_i + i\hat{p}_i), \quad \hat{a}_i^\dagger = \frac{1}{\sqrt{2}}(\hat{q}_i - i\hat{p}_i). \quad (4)$$

The number operator for the ith mode and total number operator for the n-mode system can be expressed as

$$\hat{N}_i = \hat{a}_i^\dagger \hat{a}_i = \frac{1}{2}(\hat{q}_i^2 + \hat{p}_i^2 - 1), \quad (5a)$$

$$\hat{N} = \sum_{i=1}^n \hat{N}_i. \quad (5b)$$

The state space known as the Hilbert space $\mathcal{H}_i$ for the ith mode is spanned by the eigenvectors $|n_i\rangle$ $\{n_i = 0, 1, \ldots, \infty\}$ of $N_i = a_i^\dagger a_i$. The combined Hilbert space $\mathcal{H}^{\otimes n} = \otimes_{i=1}^n \mathcal{H}_i$ of the n-mode state is spanned by the product basis vector $|n_1 \cdots n_i \cdots n_n\rangle$ with $\{n_1, \ldots, n_i, \ldots, n_n = 0, 1, \ldots, \infty\}$. The numbers n_i correspond to photon number in the ith mode. The irreducible action of the field operators $\hat{a}_i$ and $\hat{a}_i^\dagger$ on $\mathcal{H}_i$ is dictated by the commutation relation in Eq. (2) and is given by

$$\hat{a}_i|n_i\rangle = \sqrt{n_i}|n_i - 1\rangle, \quad n_i \geqslant 1, \ \hat{a}_i|0\rangle = 0,$$
$$\hat{a}_i^\dagger|n_i\rangle = \sqrt{n_i + 1}|n_i + 1\rangle, \quad n_i \geqslant 0. \quad (6)$$

We define the displacement operator acting on the ith mode and the corresponding coherent states as

$$\hat{D}_i(q_i, p_i) = e^{i(p_i\hat{q}_i - q_i\hat{p}_i)},$$
$$|q_i, p_i\rangle_i = \hat{D}_i(q_i, p_i)|0\rangle_i. \quad (7)$$

Here q_i and p_i correspond to displacement along $\hat{q}$ and $\hat{p}$ quadrature of the ith mode.

A. Symplectic transformations

The group $\mathrm{Sp}(2n, \mathcal{R})$ is defined as the group of linear homogeneous transformations S specified by real $2n \times 2n$ matrices S acting on the quadrature variables and preserving the canonical commutation relation in Eq. (2):

$$\hat{\xi}_i \rightarrow \hat{\xi}_i' = S_{ij}\hat{\xi}_j, \quad S\Omega S^T = \Omega. \quad (8)$$

The unitary representation of this group turns out to be infinite dimensional, where we have $\mathcal{U}(S)$ for each $S \in \mathrm{Sp}(2n, \mathcal{R})$ acting on a Hilbert space, and is known as the metaplectic representation. These unitary transformations are generated by Hamiltonians which are quadratic functions of quadrature and field operators. Furthermore, any symplectic matrix $S \in \mathrm{Sp}(2n, \mathcal{R})$ can be decomposed as

$$S = P \cdot T, \quad (9)$$

where $P \in \Pi(n)$ is a subset of $\mathrm{Sp}(2n, \mathcal{R})$ defined as

$$\Pi(n) = \{S \in \mathrm{Sp}(2n, \mathcal{R}) \,|\, S^T = S, \ S > 0\}, \quad (10)$$

and T is an element of $K(X, Y)$, the maximal compact subgroup of $\mathrm{Sp}(2n, \mathcal{R})$ which is isomorphic to the unitary group $U(n) = X + iY$ in n dimensions. The action of $U(n)$ transformation on the annihilation and creation operators is given as

$$\hat{\boldsymbol{a}} \rightarrow U\hat{\boldsymbol{a}}, \quad \hat{\boldsymbol{a}}^\dagger \rightarrow U^*\hat{\boldsymbol{a}}^\dagger, \quad (11)$$

where $\hat{\boldsymbol{a}} = (\hat{a}_1, \hat{a}_2, \ldots, \hat{a}_n)^T$ and $\hat{\boldsymbol{a}}^\dagger = (\hat{a}_1^\dagger, \hat{a}_2^\dagger, \ldots, \hat{a}_n^\dagger)^T$. The $2n \times 2n$ dimensional symplectic transformation matrix $K(X, Y)$ acting on the Hermitian quadrature operators can be easily obtained using Eqs. (4) and (11).

Now we write three basic symplectic operations which are used later.

1. Phase-change operation

The symplectic transformation for a phase-change operation acting on the quadrature operators $\hat{q}_i, \hat{p}_i$ is

$$R_i(\phi) = \begin{pmatrix} \cos\phi & \sin\phi \\ -\sin\phi & \cos\phi \end{pmatrix}. \quad (12)$$

This operation corresponds to the $U(1)$ subgroup of $\mathrm{Sp}(2, \mathcal{R})$, its metaplectic representation is generated by the Hamiltonian of the form $H = \hat{a}_i^\dagger \hat{a}_i$, and its action on the annihilation operator is $\hat{a}_i \rightarrow e^{-i\phi}\hat{a}_i$.

2. Single-mode squeezing operation

The symplectic transformation for the single-mode squeezing operator acting on quadrature operators $\hat{q}_i$ and $\hat{p}_i$ is written as

$$S_i(r) = \begin{pmatrix} e^{-r} & 0 \\ 0 & e^r \end{pmatrix}. \quad (13)$$

3. Beam-splitter operation

For two-mode systems with quadrature operators $\hat{\xi} = (\hat{q}_i, \hat{p}_i, \hat{q}_j, \hat{p}_j)^T$ the beam-splitter transformation $B_{ij}(\theta)$ acts as follows:

$$B_{ij}(\theta) = \begin{pmatrix} \cos\theta \, \mathbb{1}_2 & \sin\theta \, \mathbb{1}_2 \\ -\sin\theta \, \mathbb{1}_2 & \cos\theta \, \mathbb{1}_2 \end{pmatrix}, \qquad (14)$$

where $\mathbb{1}_2$ represents a 2×2 identity matrix and transmittivity is specified through θ via the relation $\tau = \cos^2\theta$. For a balanced (50:50) beam splitter, $\theta = \pi/4$. All three operations above are generated by quadratic Hamiltonians. It turns out that while phase-change and beam-splitter operations are compact and are generated by a photon-number-conserving Hamiltonian, squeezing operations are noncompact and are generated by a photon-number-nonconserving Hamiltonian.

B. Phase-space description

For a density operator $\hat{\rho}$ of a quantum system the corresponding Wigner distribution is defined as

$$W(\xi) = \frac{1}{(2\pi)^n} \int d^n q' \left\langle q - \frac{1}{2}q' \middle| \hat{\rho} \middle| q + \frac{1}{2}q' \right\rangle \exp(i q'^T \cdot p), \tag{15}$$

where $\xi = (q_1, p_1, \ldots, q_n, p_n)^T$, $q' \in \mathcal{R}^n$ and $q = (q_1, q_2, \ldots, q_n)^T$, $p = (p_1, p_2, \ldots, p_n)^T$. Therefore, $W(\xi)$ depends upon $2n$ real phase-space variables.

For an n-mode system, the first-order moments are defined as

$$d = \langle \hat{\xi} \rangle = \text{Tr}[\hat{\rho}\hat{\xi}], \tag{16}$$

and the second-order moments are best represented by the real symmetric $2n\times2n$ covariance matrix defined as

$$V = (V_{ij}) = \frac{1}{2}\langle\{\Delta\hat{\xi}_i, \Delta\hat{\xi}_j\}\rangle, \tag{17}$$

where $\Delta\hat{\xi}_i = \hat{\xi}_i - \langle\hat{\xi}_i\rangle$, and $\{,\}$ denotes an anticommutator. The number of independent real parameters required to specify the covariance matrix is $n(2n+1)$. The uncertainty principle in terms of covariance matrix reads $V + \frac{i}{2}\Omega \geqslant 0$, which implies that the covariance matrix is positive definite, i.e., $V > 0$.

A state is called a Gaussian state if the corresponding Wigner distribution is a Gaussian. Gaussian states are completely determined by their first- and second-order moments and thus we require a total of $2n + n(2n+1) = 2n^2 + 3n$ parameters to completely determine an n-mode Gaussian state. For the special case of Gaussian states, Eq. (15) can be written as [1]

$$W(\xi) = \frac{\exp[-(1/2)(\xi - d)^T V^{-1}(\xi - d)]}{(2\pi)^n \sqrt{\det V}}, \tag{18}$$

where V is the covariance matrix and d denotes the displacement of the Gaussian state in phase space.

We now compute averages of a few quantities that are required later, using the phase-space representation. Here

$$\hat{N} = \sum_{j=1}^{n} \hat{N}_i = \frac{1}{2}\sum_{j=1}^{n}(\hat{q}_i^2 + \hat{p}_i^2 - 1) \tag{19}$$

is symmetrically ordered in $\hat{q}$ and $\hat{p}$ operators; therefore, the average number of photons, $\langle\hat{N}\rangle$, for an n-mode Gaussian state can be readily computed using the Wigner distribution as follows [13,32]:

$$\langle\hat{N}\rangle = \frac{1}{2}\sum_{j=1}^{n}\int d^{2n}\xi(q_i^2 + p_i^2 - 1)W(\xi),$$

$$= \frac{1}{2}\left[\text{Tr}\left(V - \frac{1}{2}\mathbb{1}_{2n}\right) + ||d||^2\right]. \tag{20}$$

Under a unitary transformation, while quantum states transform in Schrödinger representation as $\rho \rightarrow \mathcal{U}\rho\mathcal{U}^\dagger$, in Heisenberg representation the number operator transforms as $\hat{N} \rightarrow \mathcal{U}^\dagger\hat{N}\mathcal{U}$. Specifically for a phase-space displacement $D(r)$, we have

$$\langle\hat{D}(r)^\dagger\hat{N}\hat{D}(r)\rangle = \frac{1}{2}\left[\text{Tr}\left(V - \frac{1}{2}\mathbb{1}_{2n}\right) + ||d + r||^2\right], \tag{21}$$

which simplifies by using Eq. (20) to

$$\langle\hat{D}(r)^\dagger\hat{N}\hat{D}(r)\rangle - \langle\hat{N}\rangle = \frac{1}{2}(||d + r||^2 - ||d||^2). \tag{22}$$

For a homogeneous symplectic transformation S, the density operator follows the metaplectic representation $\mathcal{U}(S)$ as $\rho \rightarrow \mathcal{U}(S)\rho\mathcal{U}(S)^\dagger$. The corresponding transformation of the displacement vector d and covariance matrix V is given by [29]

$$d \rightarrow Sd \quad \text{and} \quad V \rightarrow SVS^T. \tag{23}$$

Thus, we can easily evaluate the average of the number operator after the state has undergone a metaplectic transformation using Eqs. (20) and (23) as

$$\langle\hat{\mathcal{U}}(S)^\dagger\hat{N}\hat{\mathcal{U}}(S)\rangle = \frac{1}{2}\text{Tr}\left(VS^TS - \frac{1}{2}\mathbb{1}_{2n}\right) + \frac{1}{2}d^TS^TSd. \tag{24}$$

Therefore,

$$\langle\hat{\mathcal{U}}(S)^\dagger\hat{N}\hat{\mathcal{U}}(S)\rangle - \langle\hat{N}\rangle = \frac{1}{2}\text{Tr}[V(S^TS - \mathbb{1}_{2n})] + \frac{1}{2}d^T(S^TS - \mathbb{1}_{2n})d. \tag{25}$$

More mathematical details are available in [29].

III. ESTIMATION OF GAUSSIAN STATES USING PHOTON-NUMBER MEASUREMENTS

In this section, we present a variant of the scheme developed in [13] where the authors have devised a scheme to estimate the mean and covariance matrix of Gaussian state using PNRDs. In our scheme, which is optimal and uses minimum optical elements, photon-number measurement is performed on the original Gaussian state as well as the transformed Gaussian state. These transformations or gates consist of displacement, phase rotation, single-mode squeezing, and beam-splitter operation denoted by $\hat{D}_i(q, p)$, $\mathcal{U}(R_i(\theta))$, $\mathcal{U}(S_i(r))$, and $\mathcal{U}(B_{ij}(\theta))$, respectively.

A. Mean estimation

We first perform photon-number measurement on the original n-mode Gaussian state giving us $\langle\hat{N}\rangle$. Then we consider two different photon-number measurements after displacing one of the quadratures $\hat{q}_i$ or $\hat{p}_i$ of the ith mode by a unit amount giving us $\langle\hat{D}_i(1, 0)^\dagger\hat{N}\hat{D}_i(1, 0)\rangle$ and
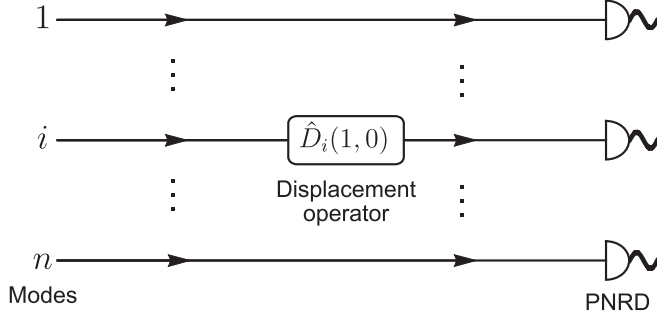
FIG. 1. To estimate the mean of an n-mode Gaussian state, the state is displaced along one of the $2n$ phase-space variables before performing photon-number measurement on each of the modes. In the figure, a displacement gate $\hat{D}_i(1, 0)$ is applied on the state which displaces the $\hat{q}$ quadrature of the ith mode by a unit amount.

FIG. 2. To estimate the intramode covariance matrix, that is, the covariance matrix of the individual modes, single-mode symplectic transformations are applied on the state before performing photon-number measurement on each of the modes. In the figure, a phase shifter $\mathcal{U}(R_i(\phi))$ followed by a squeezer $\mathcal{U}(S_i(r))$ is applied on the ith mode of the state.

$\hat{D}_i(0, 1)^{\dagger} \hat{N} \hat{D}_i(0, 1)\rangle$. (Figure 1 depicts a displacement gate $\hat{D}_i(1, 0)$ acting on the ith mode of the state.) We therefore have, by using Eq. (22),

$$\langle \hat{D}_i(1, 0)^{\dagger} \hat{N} \hat{D}_i(1, 0)\rangle - \langle \hat{N} \rangle = \tfrac{1}{2}\big(1 + 2d_{q_i}\big),$$

$$\langle \hat{D}_i(0, 1)^{\dagger} \hat{N} \hat{D}_i(0, 1)\rangle - \langle \hat{N} \rangle = \tfrac{1}{2}\big(1 + 2d_{p_i}\big), \quad (26)$$

which can be rewritten as

$$d_{q_i} = \langle \hat{D}_i(1, 0)^{\dagger} \hat{N} \hat{D}_i(1, 0)\rangle - \langle \hat{N} \rangle - \tfrac{1}{2},$$

$$d_{p_i} = \langle \hat{D}_i(0, 1)^{\dagger} \hat{N} \hat{D}_i(0, 1)\rangle - \langle \hat{N} \rangle - \tfrac{1}{2}. \quad (27)$$

Thus, we can obtain the mean values of $\hat{q}_i$ and $\hat{p}_i$ quadratures once the values of $\langle \hat{D}_i(1, 0)^{\dagger} \hat{N} \hat{D}_i(1, 0)\rangle$, $\langle \hat{D}_i(0, 1)^{\dagger} \hat{N} \hat{D}_i(0, 1)\rangle$, and $\langle \hat{N} \rangle$ have been obtained. These estimations involve measuring averages and thus require us to repeat the measurement many times.

Therefore, to obtain all the $2n$ elements of mean $\boldsymbol{d}$ of the Gaussian state, we need to perform $2n$ photon-number measurements after displacing the state by a unit amount along $2n$ different phase-space variables along with photon-number measurement on the original state. We also note that $\text{Tr}(V)$ can be obtained using Eq. (20) once the mean $\boldsymbol{d}$ of the Gaussian state has been obtained:

$$\text{Tr}(V) = 2\langle \hat{N} \rangle - ||\boldsymbol{d}||^2 + n. \quad (28)$$

Thus, we are able to estimate $2n$ elements of the mean $\boldsymbol{d}$ of the Gaussian state and the trace of the covariance matrix $\text{Tr}(V)$ using a total of $2n + 1$ photon-number measurements.

B. Estimation of intramode covariance matrix

For convenience in representation, we express the covariance matrix of the n-mode Gaussian state as follows:

$$V = \begin{pmatrix} V_{1,1} & V_{1,2} & \cdots & V_{1,n} \\ V_{2,1} & \ddots & \ddots & \vdots \\ \vdots & \ddots & \ddots & V_{n-1,n} \\ V_{n,1} & \cdots & V_{n,n-1} & V_{n,n} \end{pmatrix}, \quad (29)$$

where $V_{i,j}$ is a 2×2 matrix. Furthermore, we represent the mean and covariance matrix of the marginal state of mode i

(or intramode covariance matrix for mode i) as

$$d_i = \begin{pmatrix} d_{q_i} \\ d_{p_i} \end{pmatrix}, \quad V_{i,i} = \begin{pmatrix} \sigma_{qq} & \sigma_{qp} \\ \sigma_{qp} & \sigma_{pp} \end{pmatrix}. \quad (30)$$

To estimate the intramode covariance matrix, consider the single-mode symplectic gate $P_i(r, \phi)$ consisting of a squeezer and phase shifter acting on the ith mode of the Gaussian state:

$$P_i(r, \phi) = S_i(r)R_i(\phi) = \begin{pmatrix} e^{-r} & 0 \\ 0 & e^r \end{pmatrix} \begin{pmatrix} \cos \phi & \sin \phi \\ -\sin \phi & \cos \phi \end{pmatrix}. \quad (31)$$

The schematic representation of $P_i(r, \phi)$ is shown in Fig. 2. When $P_i(r, \phi)$ acts on the ith mode of the Gaussian state, Eq. (25) reduces to

$$\langle \hat{\mathcal{U}}(P_i)^{\dagger} \hat{N} \hat{\mathcal{U}}(P_i)\rangle - \langle \hat{N} \rangle = \tfrac{1}{2}\text{Tr}\big[V_{i,i}\big(P_i^T P_i - \mathbb{1}_2\big)\big]$$

$$+ \tfrac{1}{2}d_i^T\big(P_i^T P_i - \mathbb{1}_2\big)d_i. \quad (32)$$

Here

$$P_i^T P_i = \begin{pmatrix} e^{-2r} \cos^2 \phi + e^{2r} \sin^2 \phi & -\sinh 2r \sin 2\phi \\ -\sinh 2r \sin 2\phi & e^{-2r} \sin^2 \phi + e^{2r} \cos^2 \phi \end{pmatrix}. \quad (33)$$

For brevity, we assume

$$P_i^T P_i - \mathbb{1}_2 = \begin{pmatrix} k_1 & k_3 \\ k_3 & k_2 \end{pmatrix}, \quad (34)$$

and thus Eq. (32) simplifies as

$$\langle \hat{\mathcal{U}}(P_i)^{\dagger} \hat{N} \hat{\mathcal{U}}(P_i)\rangle - \langle \hat{N} \rangle = \tfrac{1}{2}\big[k_1 \sigma_{qq} + k_2 \sigma_{pp} + 2k_3 \sigma_{qp}$$

$$+ k_1 d_{q_i}^2 + k_2 d_{p_i}^2 + 2k_3 d_{q_i} d_{p_i}\big]. \quad (35)$$

Rearranging the above equation, we obtain

$$k_1 \sigma_{qq} + k_2 \sigma_{pp} + 2k_3 \sigma_{qp} = 2(\langle \hat{\mathcal{U}}(P_i)^{\dagger} \hat{N} \hat{\mathcal{U}}(P_i)\rangle - \langle \hat{N} \rangle)$$

$$- \big(k_1 d_{q_i}^2 + k_2 d_{p_i}^2 + 2k_3 d_{q_i} d_{p_i}\big). \quad (36)$$

Since d_{q_i} and d_{p_i} have already been obtained in Sec. III A [Eq. (27)], the above equation contains three unknown parameters σ_{qq}, σ_{pp}, and σ_{qp}. We can determine these three

unknowns by performing three distinct photon-number measurements for appropriate combinations of squeezing parameter r and phase rotation angle ϕ, as follows:

(i) For $e^r = \sqrt{2}$ and $\phi = 0$, we obtain

$$-\frac{1}{2}(\sigma_{qq} - 2\sigma_{pp}) = c_1. \qquad (37)$$

(ii) For $e^r = \sqrt{3}$ and $\phi = 0$, we obtain

$$-\frac{2}{3}(\sigma_{qq} - 3\sigma_{pp}) = c_2. \qquad (38)$$

(iii) For $e^r = \sqrt{2}$ and $\phi = \pi/4$, we obtain

$$\frac{1}{4}(\sigma_{qq} + \sigma_{pp} - 6\sigma_{qp}) = c_3. \qquad (39)$$

Here c_1, c_2, and c_3 correspond to the right-hand side (RHS) of Eq. (36), which can be easily determined once the photon-number measurements have been performed. Equations (37) and (38) can be solved to yield values of σ_{qq} and σ_{pp} which can be put in Eq. (39) to obtain the value of σ_{qp}. Thus, $V_{i,i}$ can be completely determined by performing three photon-number measurements after applying the three distinct single-mode symplectic gates [Eqs. (37)–(39)]. To determine all $V_{i,i}$ ($1 \leqslant i \leqslant n-1$), we require $3(n-1)$ measurements. For $V_{n,n}$, we need to determine σ_{qp} and one of σ_{qq} or σ_{pp}, as $\mathrm{Tr}(V)$ is already known. Thus, a total of $3(n-1) + 2 = 3n - 1$ distinct photon-number measurements are required to determine all the parameters of the intramode covariance matrix of a Gaussian state.

C. Estimation of intermode correlations matrix

To estimate the intermode correlations matrix, we perform two-mode symplectic operations on the Gaussian state before measuring photon-number distribution. We write the covariance matrix of the reduced state of the i, j mode in accord with Eq. (29) as

$$\begin{pmatrix} V_{i,i} & V_{i,j} \\ V_{i,j}^T & V_{j,j} \end{pmatrix}. \qquad (40)$$

Here $i < j$ need not be successive modes. Since $V_{i,i}$ and $V_{j,j}$ have already been determined in Sec. III B, we need to determine only $V_{i,j}$. We further take the matrix elements of $V_{i,j}$ to be

$$V_{i,j} = \begin{pmatrix} \gamma_{qq} & \gamma_{qp} \\ \gamma_{pq} & \gamma_{pp} \end{pmatrix}. \qquad (41)$$

The two-mode symplectic gate is comprised of a phase shifter acting on the ith mode followed by a balanced beam splitter acting on modes i and j and finally a squeezer acting on mode i. We represent this mathematically as

$$Q_{ij}(r, \phi) = (S_i(r) \oplus \mathbb{1}_2) B_{ij}\left(\frac{\pi}{4}\right)(R_i(\phi) \oplus \mathbb{1}_2),$$

$$= \begin{pmatrix} S_i(r) & 0 \\ 0 & \mathbb{1}_2 \end{pmatrix} \frac{1}{\sqrt{2}} \begin{pmatrix} \mathbb{1}_2 & \mathbb{1}_2 \\ -\mathbb{1}_2 & \mathbb{1}_2 \end{pmatrix} \begin{pmatrix} R_i(\phi) & 0 \\ 0 & \mathbb{1}_2 \end{pmatrix}. \qquad (42)$$

The schematic representation of $Q_{ij}(r, \phi)$ is illustrated in Fig. 3. When the aforementioned gate $Q_{ij}(r, \phi)$ acts on the
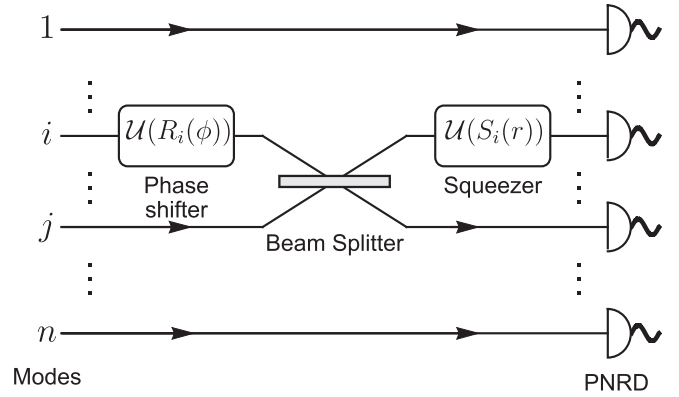
FIG. 3. To estimate the intermode correlations matrix, we apply a two-mode symplectic gate on the state before performing a photon-number measurement on each of the modes. As shown in the figure, first a phase shifter $\mathcal{U}(R_i(\phi))$ is applied on the ith mode of the state. This is followed by a balanced beam splitter $\mathcal{U}(B_{ij}(\frac{\pi}{4}))$ acting on i, j modes and finally a squeezer $\mathcal{U}(S_i(r))$ is applied on the ith mode of the state.

modes i and j of the Gaussian state, Eq. (25) reduces to

$$\langle \hat{\mathcal{U}}(Q_{ij})^\dagger \hat{N} \hat{\mathcal{U}}(Q_{ij}) \rangle - \langle \hat{N} \rangle$$
$$= \frac{1}{2}\mathrm{Tr}\left[\begin{pmatrix} V_{i,i} & V_{i,j} \\ V_{i,j}^T & V_{j,j} \end{pmatrix} \begin{pmatrix} K - \mathbb{1}_2 & M \\ M^T & L - \mathbb{1}_2 \end{pmatrix} \right]$$
$$+ \frac{1}{2} \begin{pmatrix} d_{q_i} \\ d_{p_i} \\ d_{q_j} \\ d_{p_j} \end{pmatrix}^T \begin{pmatrix} K - \mathbb{1}_2 & M \\ M^T & L - \mathbb{1}_2 \end{pmatrix} \begin{pmatrix} d_{q_i} \\ d_{p_i} \\ d_{q_j} \\ d_{p_j} \end{pmatrix}, \qquad (43)$$

where we have used

$$Q_{ij}^T Q_{ij} = \begin{pmatrix} K & M \\ M^T & L \end{pmatrix}. \qquad (44)$$

Using the following simplification for trace,

$$\mathrm{Tr}\left[\begin{pmatrix} V_{i,i} & V_{i,j} \\ V_{i,j}^T & V_{j,j} \end{pmatrix} \begin{pmatrix} K - \mathbb{1}_2 & M \\ M^T & L - \mathbb{1}_2 \end{pmatrix} \right]$$
$$= \mathrm{Tr}[V_{i,i}(K - \mathbb{1}_2) + V_{j,j}(L - \mathbb{1}_2)] + 2\mathrm{Tr}[V_{i,j}M^T], \quad (45)$$

Eq. (43) can be rearranged as

$$\mathrm{Tr}[V_{i,j}M^T] = \langle \hat{\mathcal{U}}(Q_{ij})^\dagger \hat{N} \hat{\mathcal{U}}(Q_{ij}) \rangle - \langle \hat{N} \rangle$$
$$- \frac{1}{2}\mathrm{Tr}[V_{i,i}(K - \mathbb{1}_2) + V_{j,j}(L - \mathbb{1}_2)]$$
$$- \frac{1}{2} \begin{pmatrix} d_{q_i} \\ d_{p_i} \\ d_{q_j} \\ d_{p_j} \end{pmatrix}^T \begin{pmatrix} K - \mathbb{1}_2 & M \\ M^T & L - \mathbb{1}_2 \end{pmatrix} \begin{pmatrix} d_{q_i} \\ d_{p_i} \\ d_{q_j} \\ d_{p_j} \end{pmatrix}. \qquad (46)$$

Various terms appearing in the RHS of the above equation, for instance $V_{i,i}$, $V_{j,j}$, d_{q_i}, d_{p_i}, d_{q_j}, d_{p_j} have already been determined. Thus the four unknowns γ_{qq}, γ_{pp}, γ_{qp}, γ_{pq} appearing on the left-hand side (LHS) of the above equation can be determined by performing four different photon number

TABLE I. Tomography of an n-mode Gaussian state by photon-number measurements.

Estimate type	Parameter number	Gaussian operations	Measurement number
Mean ($\boldsymbol{d}$)	$2n$	Displacement	$2n+1$
Intramode covariance ($V_{i,i}$)	$3n$	Phase shifter, squeezer	$3n-1$
Intermode correlations ($V_{i,j}$)	$2n(n-1)$	Phase shifter, squeezer, beam splitter	$2n(n-1)$
Total	$2n^2+3n$		$2n^2+3n$

measurements for appropriate combinations of squeezing parameter r and phase rotation angle ϕ. Further, LHS of Eq. (46) can be expressed as the following:

$$\text{Tr}[V_{i,j}M^T] = \tfrac{1}{2}[(e^{-2r}-1)\cos\phi\,\gamma_{qq} + (e^{2r}-1)\cos\phi\,\gamma_{pp}$$
$$+(1-e^{2r})\sin\phi\,\gamma_{qp} + (e^{-2r}-1)\sin\phi\,\gamma_{pq}]. \tag{47}$$

We take these four different combinations of squeezing parameter r and phase rotation angle ϕ to determine the four unknowns:

(i) For $e^r=\sqrt{2}$ and $\phi=0$, we obtain

$$-\tfrac{1}{4}(\gamma_{qq}-2\gamma_{pp}) = d_1. \tag{48}$$

(ii) For $e^r=\sqrt{3}$ and $\phi=0$, we obtain

$$-\tfrac{1}{3}(\gamma_{qq}-3\gamma_{pp}) = d_2. \tag{49}$$

(iii) For $e^r=\sqrt{2}$ and $\phi=\pi/2$, we obtain

$$-\tfrac{1}{4}(2\gamma_{qp}+\gamma_{pq}) = d_3. \tag{50}$$

(iv) For $e^r=\sqrt{3}$ and $\phi=\pi/2$, we obtain

$$-\tfrac{1}{3}(3\gamma_{qp}+\gamma_{pq}) = d_4. \tag{51}$$

Here d_1, d_2, d_3, and d_4 are the RHS of Eq. (46), which can be easily determined once the photon-number measurements have been performed. Equations (48) and (49) can be solved to yield values of γ_{qq} and γ_{pp}, whereas Eqs. (50) and (51) can be solved to yield values of γ_{qp} and γ_{pq}. Thus, we have used four distinct measurements to determine the four parameters of $V_{i,j}$. The intermode correlations of the Gaussian states thus require $4 \times n(n-1)/2 = 2n(n-1)$ measurements. So the total number of distinct measurements required to determine all the $2n^2+3n$ parameters of the n-mode Gaussian state adds up to $2n^2+3n$. The results are summarized in Table I. Thus, our tomography scheme for the Gaussian state using photon-number measurement is optimal in the sense that we require exactly the same number of distinct measurements as the number of independent real parameters of the Gaussian state.

IV. CHARACTERIZATION OF GAUSSIAN CHANNELS

In this section, we move on to the characterization of a Gaussian channel using coherent-state probes [14,15,17] by employing the tomography techniques developed in Sec. III. Gaussian channels are defined as those channels which transform Gaussian states into Gaussian states [25,26]. An n-mode Gaussian channel is specified by a pair of $2n \times 2n$ real matrices A and B with $B = B^T \geqslant 0$ [24]. The matrices A and B are described by a total of $4n^2 + 2n(2n+1)/2 = 6n^2 + n$

real parameters and satisfy complete positivity and a trace-preserving condition

$$B + i\Omega - iA\Omega A^T \geqslant 0. \tag{52}$$

The action of the Gaussian channel on mean $\boldsymbol{d}$ and covariance matrix V of a Gaussian state is given by

$$\boldsymbol{d} \to A\boldsymbol{d}, \quad V \to AVA^T + \tfrac{1}{2}B. \tag{53}$$

Here again we follow the scheme proposed in [13]. A schematic diagram is shown in Fig. 4. We prepare $2n$ distinct coherent-state probes by displacing the n-mode vacuum state by a unit amount along any of the $2n$ different phase-space variables. These coherent-state probes are sent through the channel and full or partial state tomography using photon-number measurement is carried out on the output states. The information about the output-state parameters enables us to characterize the Gaussian channel. Now we describe the exact scheme in detail. For convenience, we define a $2n$-dimensional column vector as

$$\boldsymbol{e}_j = (0, 0, \ldots, 1, \ldots, 0, 0)^T, \tag{54}$$

with 1 present at the jth position. The first set of n coherent-state probes is prepared by displacing an n-mode vacuum state ($\boldsymbol{d}=0$, $V=\mathbb{1}_{2n}/2$) by a unit amount along n different $\hat{q}$ quadratures. For instance, application of a displacement operator $\hat{D}_j(1,0)$ on the jth mode of the n-mode vacuum state yields the coherent state

$$|\boldsymbol{e}_{2j-1}\rangle = \hat{D}_j(1,0)|\boldsymbol{0}\rangle, \tag{55}$$
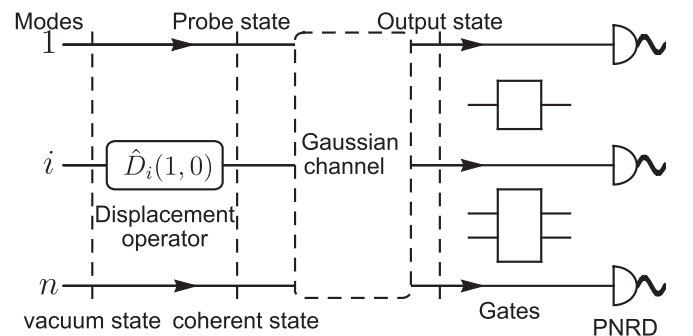
FIG. 4. Scheme for a complete characterization of an n-mode Gaussian channel. We send $2n$ distinct coherent-state probes through the channel and full or partial state tomography is carried out on the output states. In the figure, the displacement operator $\hat{D}_i(1,0)$ displaces the $\hat{q}$ quadrature of the ith mode by a unit amount of an n-mode vacuum state to give one of the required probe states. Single- and two-mode gate operations involved in state tomography and described in Sec. III are indicated as "Gates."

where $|0\rangle$ denotes an n-mode vacuum state. The mean and covariance matrix of the coherent state $|e_{2j-1}\rangle$ are given by

$$\boldsymbol{d} = \boldsymbol{e}_{2j-1}, \quad V = \tfrac{1}{2}\mathbb{1}_{2n}. \tag{56}$$

This coherent state is sent through the Gaussian channel and the mean and covariance matrix of the probe state transform according to Eq. (53):

$$\boldsymbol{d}_G = A\boldsymbol{e}_{2j-1}, \quad V_G = \tfrac{1}{2}(AA^T + B). \tag{57}$$

Now we perform full state tomography on the output state ρ_G ($j = 1$) which requires $2n^2 + 3n$ measurements. This provides us the matrix $AA^T + B$ and the first column of matrix A. For the remaining $n - 1$ probe states ($2 \leqslant j \leqslant n$), we measure only the mean of the output state ρ_G which enables us to determine all the odd columns of matrix A.

However, as we noticed in Sec. III A, we need to perform $2n + 1$ measurements to obtain the $2n$ elements of the mean vector $\boldsymbol{d}_G$. This leads to overshooting of the required number of measurements compared to the number of channel parameters for the complete characterization of the Gaussian channel, which renders the scheme nonoptimal. However, as we can see from Eq. (57), $\mathrm{Tr}(V) = \mathrm{Tr}(AA^T + B)/2$ is same for all probe states as all the output states have the same covariance matrix and has already been obtained in the process of tomography of the first output state ($j = 1$). Now we show how this fact can be exploited to obtain the value of $\langle \hat{N} \rangle$ for the other coherent-state probes, resulting in an optimal characterization of the Gaussian channel. We perform $2n$ measurements after displacing the output state ρ_G corresponding to a second coherent-state probe and obtain $2n$ equations as follows:

$$d_{q_i} = \langle \hat{D}_i(1,0)^\dagger \hat{N} \hat{D}_i(1,0) \rangle - \langle \hat{N} \rangle - \tfrac{1}{2}, \quad 1 \leqslant i \leqslant n,$$

$$d_{p_i} = \langle \hat{D}_i(0,1)^\dagger \hat{N} \hat{D}_i(0,1) \rangle - \langle \hat{N} \rangle - \tfrac{1}{2}, \quad 1 \leqslant i \leqslant n. \tag{58}$$

We substitute d_{q_i} and d_{p_i} ($1 \leqslant i \leqslant n$) in Eq. (28) and obtain a quadratic equation in $\langle \hat{N} \rangle$. After solving for $\langle \hat{N} \rangle$, we put its value in Eq. (58) to obtain d_{q_i} and d_{p_i} ($1 \leqslant i \leqslant n$). Thus, for other output states ρ_G ($2 \leqslant j \leqslant n$), only $2n$ measurements are required to determine the mean vector $\boldsymbol{d}_G$ and no additional measurements are required.

The other set of n coherent-state probes is prepared by displacing the n-mode vacuum state by a unit amount along n

different $\hat{p}$ quadratures. For instance, application of displacement operator $\hat{D}_j(0, 1)$ on the jth mode of the n-mode vacuum state yields the coherent state

$$|e_{2j}\rangle = \hat{D}_j(0,1)|\boldsymbol{0}\rangle. \tag{59}$$

The mean and covariance matrix of the coherent state $|e_{2j}\rangle$ are given by

$$\boldsymbol{d} = \boldsymbol{e}_{2j}, \quad V = \tfrac{1}{2}\mathbb{1}_{2n}. \tag{60}$$

This coherent state is sent through the Gaussian channel and the mean and covariance matrix of the probe state transform according to Eq. (53):

$$\boldsymbol{d}_G = A\boldsymbol{e}_{2j}, \quad V_G = \tfrac{1}{2}(AA^T + B). \tag{61}$$

For all these n output states ρ_G ($1 \leqslant j \leqslant n$), we measure only the mean, which enables us to determine all the even columns of matrix A. This information completely specifies matrix A as odd columns had already been determined using the first set of $\hat{q}$-displaced n coherent-state probes. This also enables us to obtain matrix B as matrix $AA^T + B$ was already known from the full state tomography on the first coherent-state probe. Thus, the total number of distinct measurements required sum up to $6n^2 + n$, as shown in Table II, which exactly coincides with the parameters specifying a Gaussian channel. In the scheme of Parthasarathy *et al.* [13], $2n - 1$ additional measurements were required which we do not need, leading to the optimality of our scheme. We note that the scheme is optimal even when the coherent-state probes have different mean values, since $\mathrm{Tr}(V)$ is the same for all the output states even in this case.

V. VARIANCE IN PHOTON-NUMBER MEASUREMENTS

In this section, we analyze the variance of photon-number distribution of the original state and gate-transformed states which we used towards state and process estimation in Secs. III and IV. This study provides us with an idea of the quality of our estimates of the Gaussian states and channels.

To evaluate the variance of photon number we note that the square of the number operator can be easily put in symmetrically ordered form as follows:

$$\hat{N}^2 = \frac{1}{4}\sum_{i,j=1}^{n}\left(\hat{q}_i^{\,2} + \hat{p}_i^{\,2} - 1\right)\left(\hat{q}_j^{\,2} + \hat{p}_j^{\,2} - 1\right),$$

$$\{\hat{N}^2\}_{\mathrm{sym}} = f(\hat{q}, \hat{p}) = \frac{1}{4}\sum_{\substack{i,\,j=1 \\ i \neq j}}^{n}\left(\hat{q}_i^{\,2} + \hat{p}_i^{\,2} - 1\right)\left(\hat{q}_j^{\,2} + \hat{p}_j^{\,2} - 1\right)$$

$$+ \frac{1}{4}\sum_{i=1}^{n}\left[\hat{q}_i^{\,4} + \hat{p}_i^{\,4} - 2\hat{q}_i^{\,2} - 2\hat{p}_i^{\,2} + \frac{1}{3}\left(\hat{q}_i^2\hat{p}_i^2 + \hat{q}_i\hat{p}_i\hat{q}_i\hat{p}_i + \hat{q}_i\hat{p}_i^2\hat{q}_i\right)\right]. \tag{62}$$

Thus, the average of $\hat{N}^2$ can be readily evaluated as

$$\langle \hat{N}^2 \rangle = \int d^{2n}\boldsymbol{\xi}\, f(q,p)W(\boldsymbol{\xi}). \tag{63}$$

TABLE II. Tomography of an n-mode Gaussian channel.

Coherent-state probe	Information obtained	Measurement number
$\hat{q}$ displaced	Odd columns of A and $(AA^T + B)$	$2n^2 + 3n + (n-1) \times 2n$
$\hat{p}$ displaced	Even columns of A	$n \times 2n$
	Total	$6n^2 + n$

Using the above equation and Eq. (20), the variance of the number operator can be written in an elegant form as [13,32,33]

$$\text{Var}(\hat{N}) = \langle \hat{N}^2 \rangle - \langle \hat{N} \rangle^2$$
$$= \tfrac{1}{2}\text{Tr}\big[\big(V - \tfrac{1}{2}\mathbb{1}_{2n}\big)\big(V + \tfrac{1}{2}\mathbb{1}_{2n}\big)\big] + \boldsymbol{d}^T V \boldsymbol{d}. \quad (64)$$

We first explore the mean and variance of photon number of a single-mode system to get some insights. We consider a single-mode Gaussian state with mean $\boldsymbol{d} = (u, u)^T$ and covariance matrix

$$V(\beta) = \tfrac{1}{2}(2\mathcal{N} + 1)R(\beta)S(2s)R(\beta)^T, \quad (65)$$

where $\mathcal{N}$ is the thermal noise parameter, s is the squeezing, and β is the phase shift angle. The mean and variance of the number operator for the above state read

$$\langle \hat{N} \rangle = \mathcal{N} \cosh 2s + \sinh^2 s + u^2,$$
$$\text{Var}(\hat{N}) = \big(\mathcal{N} + \tfrac{1}{2}\big)^2 \cosh 4s - \tfrac{1}{4}$$
$$+ 2u^2\big(\mathcal{N} + \tfrac{1}{2}\big)(\cosh 2s + \sin 2\beta \sinh 2s). \quad (66)$$

Here both mean and variance depend on displacement u and squeezing s of the state. However, the mean photon number is independent of the phase shift angle β while the variance of the photon number depends on β. The variance of the displaced number operator is given by

$$\text{Var}(\hat{D}(\boldsymbol{r})^\dagger \hat{N} \hat{D}(\boldsymbol{r})) = (\boldsymbol{d} + \boldsymbol{r})^T V (\boldsymbol{d} + \boldsymbol{r})$$
$$+ \tfrac{1}{2}\text{Tr}\big[\big(V - \tfrac{1}{2}\mathbb{1}_{2n}\big)\big(V + \tfrac{1}{2}\mathbb{1}_{2n}\big)\big]. \quad (67)$$

In Fig. 5(a), we plot $\langle \hat{N} \rangle$ and $\langle \hat{D}^\dagger(1, 0)\hat{N}\hat{D}(1, 0) \rangle$ as a function of displacement parameter u for a single-mode squeezed coherent thermal state (65). We see that while $\langle \hat{D}^\dagger(1, 0)\hat{N}\hat{D}(1, 0) \rangle$ is larger than $\langle \hat{N} \rangle$, the mean values of both the operators increase with the displacement parameter u. Furthermore, $\langle \hat{D}^\dagger(1, 0)\hat{N}\hat{D}(1, 0) \rangle$ equals $\langle \hat{D}^\dagger(0, 1)\hat{N}\hat{D}(0, 1) \rangle$ as can be seen from Eq. (21). Similarly, Fig. 5(b) shows that mean values $\langle \hat{N} \rangle$ and $\langle \hat{D}^\dagger(1, 0)\hat{N}\hat{D}(1, 0) \rangle$ increase with squeezing s. We plot the variance of the operators $\hat{N}$ and $\hat{D}^\dagger(1, 0)\hat{N}\hat{D}(1, 0)$ as a function of displacement parameter u in Fig. 5(c). We see that while the variance of operator $\hat{D}^\dagger(1, 0)\hat{N}\hat{D}(1, 0)$ is larger than the variance of the operator $\hat{N}$, the variance of both the operators increases with displacement parameter u. Similarly, Fig. 5(d) shows that variance of the operators $\hat{N}$ and $\hat{D}^\dagger(1, 0)\hat{N}\hat{D}(1, 0)$ increases with squeezing s.

The variance of photon number after a symplectic transformation S of the state reads as

$$\text{Var}(\mathcal{U}(S)^\dagger \hat{N} \mathcal{U}(S))$$
$$= \boldsymbol{d}^T V \boldsymbol{d} + \tfrac{1}{2}\text{Tr}\big[\big(SVS^T - \tfrac{1}{2}\mathbb{1}_{2n}\big)\big(SVS^T + \tfrac{1}{2}\mathbb{1}_{2n}\big)\big]. \quad (68)$$

Using this expression we first compare the variance of the number operator under the action of the $P_i(r, \phi)$ gate [Eq. (31)] for different values of the parameters r and ϕ. In Fig. 6(a), we plot the variance of different $P_i(r, \phi)$ gate-transformed number operators as a function of displacement u for the single-mode squeezed coherent thermal state (65). We can see that the variance of different $P_i(r, \phi)$ gate-transformed number operators increases with displacement u. While the variance of $\mathcal{U}^\dagger(P)\hat{N}\mathcal{U}(P)$ with $e^r = \sqrt{2}$, $\phi = \pi/4$ is always lower than the variance of $\hat{N}$ and the variance of $\mathcal{U}^\dagger(P)\hat{N}\mathcal{U}(P)$ with $e^r = \sqrt{3}$, $\phi = 0$ is always higher than the variance of $\hat{N}$, the variance of $\mathcal{U}^\dagger(P)\hat{N}\mathcal{U}(P)$ with $e^r = \sqrt{2}$, $\phi = 0$ crosses over the variance of $\hat{N}$ at a certain value of displacement u. We show the variance of the photon number as a function of squeezing parameter s in Fig. 6(b). As we can see, variance of different $P_i(r, \phi)$ gate-transformed number operators shows a similar dependence on squeezing s as that of displacement u.

Now to compare the variance of photon number under the action of two mode gates $Q_{ij}(r, \phi)$ [Eq. (42)], we consider a two-mode Gaussian state with mean $\boldsymbol{a} = (u, u, u, u)^T$ and covariance matrix V,

$$V = B_{12}\left(\frac{\pi}{4}\right)[V(\beta_1) \oplus V(\beta_2)]B_{12}\left(\frac{\pi}{4}\right)^T, \quad (69)$$

where $V(\beta)$ is defined in Eq. (65). We use Eq. (68) to compute the variance of the $Q_{ij}(r, \phi)$ gate-transformed number operator corresponding to the above state.
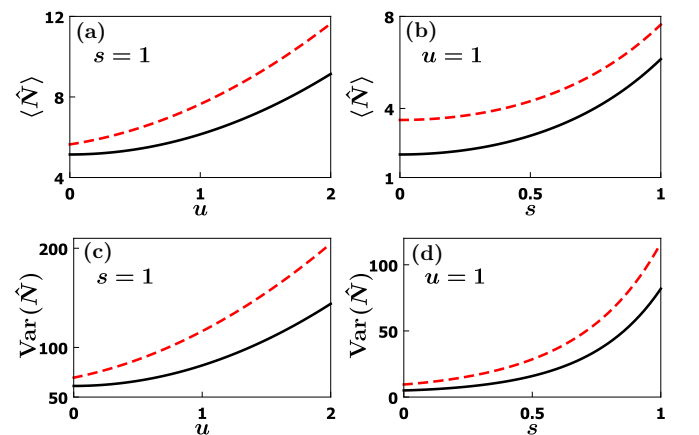
FIG. 5. Single-mode squeezed coherent thermal state (65) has been plotted with parameters $\beta = \pi/3$ and $\mathcal{N} = 1$. For all four panels, the solid black curve represents mean and variance of $\hat{N}$, while the dashed red curve represents mean and variance of $\hat{D}^\dagger(1, 0)\hat{N}\hat{D}(1, 0)$. (a) Mean photon number as a function of displacement u. (b) Mean photon number as a function of squeezing s. (c) Variance of photon number as a function of displacement u. (d) Variance of photon number as a function of squeezing s.
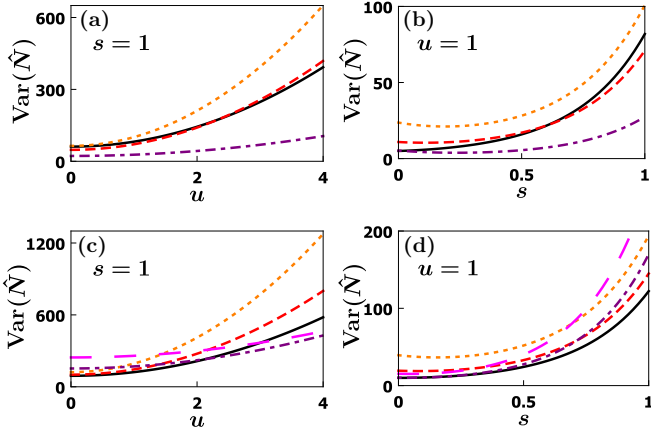
FIG. 6. (a) Variance of photon number as a function of displacement u for single-mode squeezed thermal state (65). (b) Variance of photon number as a function of squeezing s for single-mode squeezed thermal state (65). For both panels (a) and (b), various curves correspond to $\text{Var}(\mathcal{U}^\dagger(P)\hat{N}\mathcal{U}(P))$ with $e^r = \sqrt{2}$, $\phi = 0$ (red dashed), $e^r = \sqrt{3}$, $\phi = 0$ (orange dotted), and $e^r = \sqrt{2}$, $\phi = \pi/4$ (purple dot dashed), while the solid black curve represents $\text{Var}(\hat{N})$, and parameter $\beta = \pi/3$. (c) Variance of photon number as a function of displacement u for two-mode squeezed thermal state (69). (d) Variance of photon number as a function of squeezing s for two-mode squeezed thermal state (69). For both panels (c) and (d), various curves correspond to $\text{Var}(\mathcal{U}^\dagger(Q)\hat{N}\mathcal{U}(Q))$ with $e^r = \sqrt{2}$, $\phi = 0$ (red dashed), $e^r = \sqrt{3}$, $\phi = 0$ (orange dotted), $e^r = \sqrt{2}$, $\phi = \pi/2$ (purple dot dashed), and $e^r = \sqrt{3}$, $\phi = \pi/2$ (magenta large dashed), while the solid black curve represents $\text{Var}(\hat{N})$. For all four panels, the thermal parameter has been taken as $\mathcal{N} = 1$.

In Fig. 6(c), we plot the variance of different $Q_{ij}(r, \phi)$ gate-transformed number operators as a function of displacement u for the two-mode squeezed coherent thermal state (69). We can see that the variance of different $Q_{ij}(r, \phi)$ gate-transformed number operators increases with displacement. While the variance of $\mathcal{U}^\dagger(Q)\hat{N}\mathcal{U}(Q)$ with $e^r = \sqrt{2}$, $\phi = 0$, and $e^r = \sqrt{3}$, $\phi = 0$ always remains higher than the variance of $\hat{N}$, the variance of $\mathcal{U}^\dagger(Q)\hat{N}\mathcal{U}(Q)$ with $e^r = \sqrt{2}$, $\phi = \pi/2$ and $e^r = \sqrt{3}$, $\phi = \pi/2$ crosses over the variance of $\hat{N}$ at a certain value of the displacement parameter u. The variance of different $Q_{ij}(r, \phi)$ gate-transformed number operators as a function of squeezing s is shown in Fig. 6(d). As we can see, the squeezing dependence of different variances exhibits a similar trend as that of dependence on displacement.

Now we wish to relate the variances of transformed number operators to the variance of estimated Gaussian parameters. For an n-mode system, quadrature operators $\hat{q}_i$ and $\hat{p}_i$ can be expressed as

$$\hat{q}_i = \hat{D}_i(1, 0)^\dagger \hat{N}\hat{D}_i(1, 0) - \hat{N} - \tfrac{1}{2},$$
$$\hat{p}_i = \hat{D}_i(0, 1)^\dagger \hat{N}\hat{D}_i(0, 1) - \hat{N} - \tfrac{1}{2}. \tag{70}$$

Averaging the above equation yields Eq. (27). Since $\hat{N}$ and $\hat{D}_i(1, 0)^\dagger \hat{N}\hat{D}_i(1, 0)$ are measured on different states, these operators are uncorrelated and the expressions for the variance of the quadratures become

$$\text{Var}(\hat{q}_i) = \text{Var}(\hat{D}_i(1, 0)^\dagger \hat{N}\hat{D}_i(1, 0)) + \text{Var}(\hat{N}),$$
$$\text{Var}(\hat{p}_i) = \text{Var}(\hat{D}_i(0, 1)^\dagger \hat{N}\hat{D}_i(0, 1)) + \text{Var}(\hat{N}). \tag{71}$$

Thus, the variance of the $\hat{q}_i$ quadrature, which represents the quality of estimation of quadrature $\hat{q}_i$, depends on both displacement u and squeezing s as we can see from the above analysis. The optimization of parameters q_i and p_i appearing in the displacement gate $D_i(q_i, p_i)$ is required in order to minimize $\text{Var}(\hat{q}_i)$.

Similarly we can express $\hat{q}_i^2$ as

$$\hat{q}_i^2 = 6\left[\underbrace{\hat{\mathcal{U}}(P_i)^\dagger \hat{N}\hat{\mathcal{U}}(P_i)}_{e^r = \sqrt{3}, \phi = 0} - 2\underbrace{\hat{\mathcal{U}}(P_i)^\dagger \hat{N}\hat{\mathcal{U}}(P_i)}_{e^r = \sqrt{2}, \phi = 0} - \hat{N}\right]. \tag{72}$$

Thus, the variance of $\hat{q}_i^2$ can be written as

$$\text{Var}(\hat{q}_i^2) = 6\left[\underbrace{\text{Var}(\hat{\mathcal{U}}(P_i)^\dagger \hat{N}\hat{\mathcal{U}}(P_i))}_{e^r = \sqrt{3}, \phi = 0} + 2\underbrace{\text{Var}(\hat{\mathcal{U}}(P_i)^\dagger \hat{N}\hat{\mathcal{U}}(P_i))}_{e^r = \sqrt{2}, \phi = 0} \right.$$
$$\left. + \text{Var}(\hat{N})\right]. \tag{73}$$

We see from the above analysis that the variance of $\hat{q}_i^2$ also depends on both displacement u and squeezing s. In this case too, a proper study of the optimization of $P_i(r, \phi)$ gate parameters for the minimization of $\text{Var}(\hat{q}_i^2)$ is needed. Such an analysis will be useful for the best estimation of Gaussian state parameters. Similarly, various intramode correlation terms such as $\text{Var}(\hat{p}_i^2)$ and $\text{Var}(\hat{q}_i\hat{p}_i)$, as well as various intermode correlation terms such as $\text{Var}(\hat{q}_i\hat{q}_j)$ and $\text{Var}(\hat{q}_i\hat{p}_j)$, can be expressed in terms of the variances of different transformed number operators.

VI. CONCLUDING REMARKS

In this work we presented a Gaussian state tomography and Gaussian process tomography scheme based on photon-number measurements. While the work builds upon the proposal given in [13], the current proposal offers an optimal solution to the problem, with a smaller number of optical elements which renders the scheme more accessible to experimentalists. After describing our optimal scheme for Gaussian state tomography, we use it for estimation of a Gaussian channel in an optimal way, where a total number of $6n^2 + n$ distinct measurements are required to determine $6n^2 + n$ parameters specifying a Gaussian channel. Here we have exploited the fact that $\text{Tr}(V)$ is the same for all the output states corresponding to coherent-state probes with the same or different mean. Full state tomography of the first coherent-state probe yields an estimation of $\text{Tr}(V)$ which can be used to estimate $\langle\hat{N}\rangle$ for each of the remaining coherent-state probes, thus making the scheme optimal. This in some sense completes the problem of finding an optimal solution of the Gaussian channel characterization posed in [13].

It should be noted that our scheme is an improvement over similar earlier schemes based on photon-number measurements and not over homodyne and heterodyne techniques which are currently more prevalent. Similarly, the optimality is in terms of the number of distinct experiments needed in the scheme while each experiment will have to be repeated to obtain the required average values. Having said so, it is worth mentioning that there have been attempts to develop homodyne measurement schemes using weak local oscillators

and PNRDs [34,35] for use in circumstances where strong local oscillators are not desirable and are essential for the traditional homodyne scheme. Our scheme based on PNRDs is an advancement in this direction as it requires no local oscillator. Homodyne and heterodyne schemes go beyond Gaussian states, whereas our present scheme is aimed only at the estimation of Gaussian states. In principle, PNRD-based tomography schemes that go beyond Gaussian states can be invented; however, this aspect requires more investigation. Finally, since PNRD measurements have become possible in recent times, it is expected that in the coming years they will become more practical and easier.

The analysis of variance in photon-number measurements of the original and transformed states shows that the variance increases with the mean of the state and with the squeezing parameter. Thus, this scheme is well suited for states with small mean values or small displacements and small values of squeezing. Extending the scheme for states with large mean value but better estimation performance is under consideration and will be reported elsewhere. While we have chosen certain specific values of gate parameters [see Eq. (37)], to extract information about the parameters of the state, the effect of different values of gate parameters on the quality of estimates, and determination of optimal parameters that maximize the performance of the scheme needs further investigation. The optimality of the procedure may have a relationship with mutually unbiased basis for the CV systems. Further analysis of this aspect will require us to go beyond Gaussian states and will be taken up elsewhere.

[1] C. Weedbrook, S. Pirandola, R. García-Patrón, N. J. Cerf, T. C. Ralph, J. H. Shapiro, and S. Lloyd, Rev. Mod. Phys. **84**, 621 (2012).

[2] G. Adesso, S. Ragy, and A. R. Lee, Open Syst. Inf. Dyn. **21**, 1440001 (2014).

[3] D. F. V. James, P. G. Kwiat, W. J. Munro, and A. G. White, Phys. Rev. A **64**, 052312 (2001).

[4] *Quantum State Estimation*, edited by M. Paris and J. Řeháček, Lecture Notes in Physics Vol. 649 (Springer-Verlag, Berlin, 2004).

[5] A. I. Lvovsky and M. G. Raymer, Rev. Mod. Phys. **81**, 299 (2009).

[6] H. P. Yuen, Phys. Lett. A **91**, 101 (1982).

[7] H. P. Yuen and V. W. S. Chan, Opt. Lett. **8**, 177 (1983).

[8] K. Vogel and H. Risken, Phys. Rev. A **40**, 2847 (1989).

[9] G. Harder, T. J. Bartley, A. E. Lita, S. W. Nam, T. Gerrits, and C. Silberhorn, Phys. Rev. Lett. **116**, 143601 (2016).

[10] J. Hloušek, M. Dudka, I. Straka, and M. Ježek, Phys. Rev. Lett. **123**, 153604 (2019).

[11] J. Fiurášek and N. J. Cerf, Phys. Rev. Lett. **93**, 063601 (2004).

[12] J. Wenger, J. Fiurášek, R. Tualle-Brouri, N. J. Cerf, and P. Grangier, Phys. Rev. A **70**, 053812 (2004).

[13] K. R. Parthasarathy and R. Sengupta, Infin. Dimens. Anal. Quantum Probab. Relat. Top. **18**, 1550023 (2015).

[14] M. Lobino, D. Korystov, C. Kupchak, E. Figueroa, B. C. Sanders, and A. I. Lvovsky, Science **322**, 563 (2008).

[15] S. Rahimi-Keshari, A. Scherer, A. Mann, A. T. Rezakhani, A. I. Lvovsky, and B. C. Sanders, New J. Phys. **13**, 013006 (2011).

[16] A. Anis and A. I. Lvovsky, New J. Phys. **14**, 105021 (2012).

[17] X.-B. Wang, Z.-W. Yu, J.-Z. Hu, A. Miranowicz, and F. Nori, Phys. Rev. A **88**, 022101 (2013).

[18] M. Cooper, E. Slade, M. Karpiński, and B. J. Smith, New J. Phys. **17**, 033041 (2015).

[19] C. Kupchak, S. Rind, B. Jordaan, and E. Figueroa, Sci. Rep. **5**, 16581 (2015).

[20] J. Fiurášek, Phys. Rev. A **92**, 022101 (2015).

[21] M. Ghalaii and A. T. Rezakhani, Phys. Rev. A **95**, 032336 (2017).

[22] L. Ruppert and R. Filip, Sci. Rep. **7**, 39641 (2017).

[23] K. V. Jacob, A. E. Mirasola, S. Adhikari, and J. P. Dowling, Phys. Rev. A **98**, 052327 (2018).

[24] T. Heinosaari, A. S. Holevo, and M. M. Wolf, Quantum Inf. Comput. **10**, 619 (2010).

[25] A. S. Holevo, *Quantum Systems, Channels, Information: A Mathematical Introduction*, De Gruyter Studies in Mathematical Physics Vol. 16 (De Gruyter, Berlin, 2012).

[26] K. R. Parthasarathy, Indian J. Pure Appl. Math. **46**, 419 (2015).

[27] D. B. S. Soh, C. Brif, P. J. Coles, N. Lütkenhaus, R. M. Camacho, J. Urayama, and M. Sarovar, Phys. Rev. X **5**, 041010 (2015).

[28] B. Qi, P. Lougovski, R. Pooser, W. Grice, and M. Bobrek, Phys. Rev. X **5**, 041009 (2015).

[29] Arvind, B. Dutta, N. Mukunda, and R. Simon, Pramana **45**, 471 (1995).

[30] S. L. Braunstein and P. van Loock, Rev. Mod. Phys. **77**, 513 (2005).

[31] G. Adesso and F. Illuminati, J. Phys. A **40**, 7821 (2007).

[32] V. V. Dodonov, O. V. Man'ko, and V. I. Man'ko, Phys. Rev. A **50**, 813 (1994).

[33] G. Vallone, G. Cariolaro, and G. Pierobon, Phys. Rev. A **99**, 023817 (2019).

[34] A. Allevi, M. Bina, S. Olivares, and M. Bondani, Int. J. Quantum Inf. **15**, 1740016 (2017).

[35] G. S. Thekkadath, D. S. Phillips, J. F. F. Bulmer, W. R. Clements, A. Eckstein, B. A. Bell, J. Lugani, T. A. W. Wolterink, A. Lita, S. W. Nam, T. Gerrits, C. G. Wade, and I. A. Walmsley, Phys. Rev. A **101**, 031801(R) (2020).